Relationship between Epithelial Organisation and Morphogen Interpretation

Dagmar Iber[1, 2, *] and Roman Vetter[1, 2]

[1] *Department of Biosystems Science and Engineering, ETH Zürich, Mattenstrasse 26, 4058 Basel, Switzerland*
[2] *Swiss Institute of Bioinformatics, Mattenstrasse 26, 4058 Basel, Switzerland*

28 February 2022

Despite molecular noise and small genetic differences between individuals, developmental outcomes are remarkably constant. Decades of research has focused on the underlying mechanisms that ensure this precision and robustness. Recent quantifications of chemical gradients and epithelial cell shapes provide novel insights into the basis of precise development. In this review, we focus on the latest developments with regard to epithelial morphogenesis.

Keywords: tissue patterning, morphogen gradient, positional error, cell shape, pseudo-stratified epithelium, cell organisation
[*]**Correspondence:** dagmar.iber@bsse.ethz.ch

Introduction

Epithelia are the first tissue type to emerge during morphogenesis. A hallmark of epithelia is apical-basal polarity (Fig. 1). Beneath the apical surface, tight junctions create a watertight seal, and control the paracellular passage of ions and solutes between epithelial cells, while preventing the mixing of apical and basal-lateral membranes. The adhesion belt and further adhesive junctions along the lateral side stabilise the cell-cell contacts. On the basal-most side, epithelia bind tightly to the basal lamina. The first epithelial structure, the blastula, is a hollow sphere made of a single epithelial cell layer. At later stages, multi-layered epithelia emerge. As development progresses, the simple epithelial sheets, tubes, and vesicles grow and deform into the complex shapes characteristic of organs and adult tissues. These morphogenetic changes are guided by a wide range of mechanisms that use chemical signals, mechanical constraints, and fluid-flow-induced shear stress. As animals develop from a single cell, cells must take on the correct fate at the right position and time to build a functional organism. Developmental outcomes are remarkably constant despite environmental, inter-individual, and evolutionary changes that alter reaction time and patterning length scales [1–3], a phenomenon coined as canalisation. How such developmental precision and robustness is achieved is still largely unknown. While mechanical contributions have recently received greater attention, precision of morphogenesis has, so far, mainly been studied for gradient-based patterning.

Morphogen Gradient Precision

The measured morphogen gradients can be approximated well either by an exponential function

$$C(x) = C_0 e^{-x/\lambda} \tag{1}$$

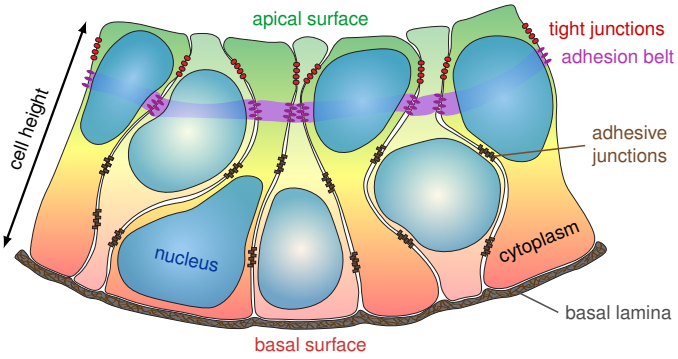

Figure 1: Cell polarity in a pseudo-stratified epithelial layer.

with an amplitude C_0 at the morphogen source at $x = 0$ and a decay length λ (Fig. 2A), or by a power law

$$C(x) = A(x + x_0)^{-m}, \tag{2}$$

where A, m, x_0 are positive constants [4–9]. These gradient profiles emerge independent of whether morphogen transport happens via diffusion or cytonemes [10]. Diffusion-based gradients have been argued to be more precise for large gradient length, and vice versa [11]. Power law gradients arise from ligand-enhanced degradation and are less sensitive to a variable source [12], but the shallower gradient profile far away from the source limits their usefulness [13]. It has been argued that the best cost-precision trade-off can be achieved when gradients are read out at about 2λ from the source [14], but patterning distances are much larger in the neural tube (NT) [7], and SHH-dependent responses are observed even in the very dorsal NT, which is more than 10λ away from the SHH source [15].

According to the French flag model, morphogen gradients define different tissue domains via concentration thresholds (Fig. 2A) [16, 17], although intracellular regulatory networks can result in more complex dependencies [18, 19]. In case of a threshold-based readout, cells exposed to morphogen concentrations above the threshold take on a different fate from cells exposed to lower concentrations. Measurements in several developmental systems reveal the direct readouts of the morphogen gradients to be smooth [7, 20, 17, 21]. Sharp transitions require highly sensitive readout mechanisms, as can arise from cooperativity, zero-order ultrasensitivity, or hysteresis. Bistable networks have been explored to explain sharp boundaries in development, and to engineer gradient-based patterning in synthetic biology approaches [22–26, 21]. Also with sharp readouts, noise can still result in a transition zone with mixed cell fates (Fig. 2B), resulting in misaligned boundaries in morphogenetic fields of single embryos. As the morphogen concentration de-

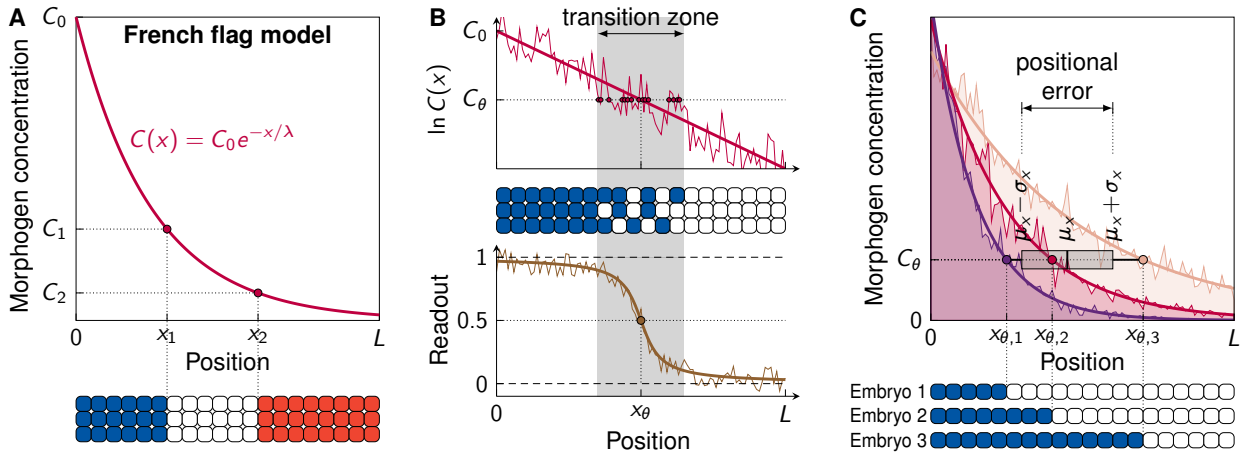

Figure 2: Morphogen gradient precision. (A) The French flag model. **(B)** Transition zones are not necessarily sharp. **(C)** Variability in the gradients translates into different readout positions. μ_x is the mean readout position of the three gradients.

clines with distance from the source, noise-driven transition zones have been suggested to widen [13]. Cell alignment along sharp boundaries can be achieved via polarised contractility, adhesion-based cell sorting and cell competition [27–32].

Deviations in the readout position, x_θ, between embryos, i, are referred to as positional error (Fig. 2C),

$$\sigma_x = \mathrm{SD}\left\{x_{\theta,i}\right\}. \tag{3}$$

The positional error has been reported to be smaller for the read-out than for the gradient [4, 33, 34, 7], resulting in a quest for the precision-enhancing mechanism. Spatial and temporal averaging have been proposed to enhance precision in the *Drosophila* blastoderm syncytium [4], and the downstream gap gene network has been suggested to act as an optimal decoder of upstream positional information by integrating maternal inputs across the embryo [35, 36]. Similarly, optimal decoding of the opposing SHH and BMP gradients has been proposed to explain the high precision of the progenitor domain boundaries in the center of the mouse NT [7]. However, the gradient variability had been overestimated, and single gradients would be precise enough to pattern the center [37].

Recent work highlights the importance of dynamics for patterning precision in the *Drosophila* blastoderm. Precise patterning can be achieved faster when cellular decision times vary depending on the statistical realisation of the noisy signal, as formulated in Wald's sequential probability ratio test [38], and the transient dynamics that emerge from the complex regulatory interactions in the gap gene network play an important role in patterning precision and canalisation [19].

As gradients are more difficult to image than their readouts, there remains the possibility that the reported higher gradient variability reflects technical errors. For the reported molecular noise levels in morphogen production, decay, and transport, cell-based simulations predict a gradient variability that is consistent with the observed precision of readouts, even at very large distances from the source [37, 39]. Morphogen gradients may thus be more precise than thought and provide sufficient positional information on their own.

Relationship between Cellular Organization and Patterning Precision

Tissues that employ gradient-based patterning have small apical surfaces [39]. Large cell diameters increase gradient variability via their impact on morphogen production, removal, and transport, while spatial averaging over the cell surface or via cilia- or cytoneme-based sensing has only a small impact in the cell-based simulations (Fig. 3A). Many ligands are sensed also on the basal-lateral side [41, 42], but the same principles that apply apically also apply basal-laterally: Also in this case, smaller cell diameters will result in less variability. As morphogens must diffuse through the tortuous inter-cellular space to reach the lateral sides, the effective diffusion path is, however, longer than the beeline [43].

A small apical surface or cell diameter is not necessarily a reflection of small overall cell size, as measured by their volume. For one, tissue curvature can result in smaller apical surfaces (Fig. 1A). In the NT, the SHH-sensing cilium is indeed located on the inner, apical surface [44], while in the flat *Drosophila* wing and eye discs, cells sense Hh along the entire apical-basal axis [42]. Several morphogens, including SHH and ligands of the TGF-β and the WNT family, have been shown to increase the apical-basal height of epithelial cells, and thus shrink the cell diameter, via their impact on actin polymerisation, myosin localisation and activity [45–47]. Morphogen signalling itself may thus result in small epithelial cell diameters—a relationship that deserves further clarification.

For small cell diameters, the nucleus—albeit deformable—is wider than the average cell diameter, and the nuclei disperse along the apical-basal axis, a phenomenon commonly referred to as pseudo-stratification [48, 40]. During mitosis, the nuclei must locate to the apical surface. As there is insufficient space to accommodate all nuclei apically, they move towards the basal side during the G1 phase, and back to the apical surface during the G2 phase in a process termed interkinetic nuclear migration (IKNM) [48]. The evolutionary driving force behind the emergence of pseudo-stratification has so far remained elusive, but may now be explicable with the importance of slim cells for high patterning precision.

Cells in pseudo-stratified epithelia change their neighbour relationships several times along the apical-basal axis in an effort to minimise the surface area that covers their complex cell shapes [40]. Cells are thus in contact with many more cells than what is apparent on the apical or basal cell surface, and potentially sense ligands over a wider distance (Fig. 3B). The neighbour relationships change dynamically over time, facilitating the sorting of epithelial cells to create sharper boundaries [40, 32]. At the same time, cells or nuclei that may appear as if they were in the "wrong" position in 2D slices may actually be in the correct domain (Fig. 3C). Going forward, it will be important to analyse expression domain boundaries in 3D. Given the fluidity of cell contacts, sharp boundaries may not be as relevant as correct progenitor cell counts. The size of interior

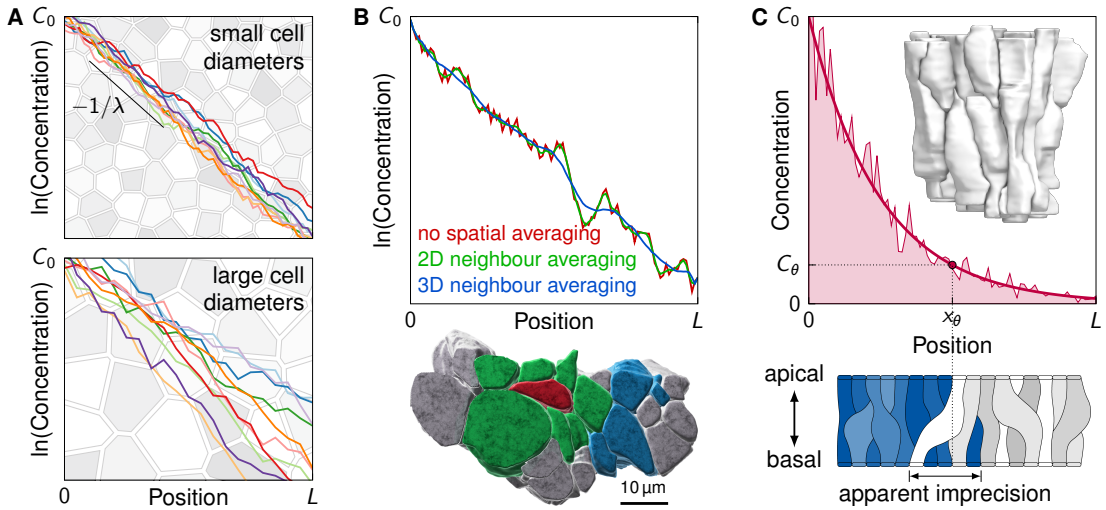

Figure 3: Relationship between cellular organization and patterning precision. **A**, Morphogen gradients across tissues with small cell diameters are less variable than with large cell diameters. **B**, Spatial concentration averaging over cell neighbourhoods reduces gradient variability only little. Long-range 3D cell contacts may increase this effect. Bottom: Non-local cell neighbourship in the mouse lung epithelium as seen on the apical surface, reproduced with modifications from [40]. Green and blue cells are in direct contact with the red cell somewhere along the apical-basal axis, even though on the surface, only green neighbours are apparent. **C**, The complex non-columnar shape of cells in pseudo-stratified epithelia my give rise to an apparent imprecision of domain boundaries (blue/white). Inset: Epithelial cells in the developing monolayer epithelium of the developing mouse lung.

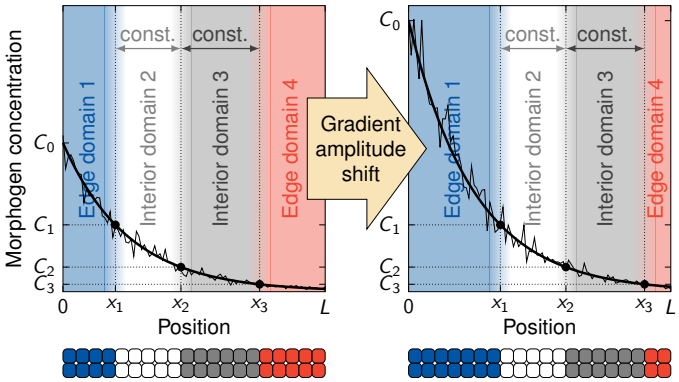

Figure 4: Precision of progenitor cell numbers. In interior patterning domains, cell numbers are preserved under changes in the amplitude of exponential morphogen gradients.

domains is more precise than the position of the domain boundaries as changes in the gradient amplitude shift the position of the domain without altering its size (Fig. 4) [37].

Conclusion & Outlook

Patterning precision has long been analysed with a focus on the information content of chemical gradients. It now becomes increasingly evident that tissues achieve high patterning precision not only by minimising molecular noise in chemical reactions, but also by controlling cell and tissue geometry [39, 2]. Mechanical stress patterns that depend on the cellular contractility and substrate stiffness may also contribute to tissue patterning [49]. Finally, tissue patterning and growth are intricately linked. Morphogens control not only patterning, cell differentiation, and cell shapes, but also the tissue growth rate [6]. How embryos control tissue size and how patterns scale with domain size remains a field of intense enquiry (e.g., [9, 50–54]). Synthetic gradients [55, 50, 56] and computational frameworks that enable high-resolution 3D cell-based tissue simulations [57] are promising tools to understand how nature achieves robust and reliable patterning to an extent that the same molecular patterning mechanism can be re-used in evolution, despite large changes in tissue size and developmental rate.

Acknowledgements

This work was funded by SNF Sinergia grant CRSII5_70930. We thank Kevin Yamauchi for helpful comments, and apologise to those authors whose work we could not discuss due to length and citation constraints.

Competing Interests

None declared.

References

[1] H. Zhu, Y. Cui, C. Luo, and F. Liu. Quantifying Temperature Compensation of Bicoid Gradients with a Fast T-Tunable Microfluidic Device. *Biophys. J.*, 119:1193–1203, 2020. doi: 10.1016/j.bpj.2020.08.003.

[2] A. Huang, J. F. Rupprecht, and T. E. Saunders. Embryonic geometry underlies phenotypic variation in decanalized conditions. *eLife*, 9:e47380, 2020. doi: 10.7554/eLife.47380.

[3] T. Rayon and J. Briscoe. Cross-species comparisons and *in vitro* models to study tempo in development and homeostasis. *Interface Focus*, 11:20200069, 2021. doi: 10.1098/rsfs.2020.0069.

[4] T. Gregor, D. W. Tank, E. F. Wieschaus, and W. Bialek. Probing the Limits to Positional Information. *Cell*, 130: 153–164, 2007. doi: 10.1016/j.cell.2007.05.025.

[5] O. Wartlick, A. Kicheva, and M González-Gaitán. Morphogen gradient formation. *Cold Spring Harb. Perspect. Biol.*, 1:a001255, 2009. doi: 10.1101/cshperspect.a001255.

[6] O. Wartlick, P. Mumcu, A. Kicheva, T. Bittig, C. Seum, F. Jülicher, and M. González-Gaitán. Dynamics of Dpp Signaling and Proliferation Control. *Science*, 331:1154–1159, 2011. doi: 10.1126/science.1200037.

[7] M. Zagorski, Y. Tabata, N. Brandenberg, M. P. Lutolf, G. Tkačik, T. Bollenbach, J. Briscoe, and A. Kicheva. Decoding of position in the developing neural tube from antiparallel morphogen gradients. *Science*, 356:1379–1383, 2017. doi: 10.1126/science.aam5887.

[8] W. K. Chan, D. J. Price, and T. Pratt. FGF8 morphogen gradients are differentially regulated by heparan sulphotransferases Hs2st and Hs6st1 in the developing brain. *Biol. Open*, 6:1933–1942, 2017. doi: 10.1242/bio.028605.

[9] R. Mateus, L. Holtzer, C. Seum, Z. Hadjivasiliou, M. Dubois, F. Jülicher, and M. González-Gaitán. BMP Signaling Gradient Scaling in the Zebrafish Pectoral Fin. *Cell Rep.*, 30:4292–4302.e7, 2020. doi: 10.1016/j.celrep.2020.03.024.

[10] A. Aguirre-Tamaral and I. Guerrero. Improving the understanding of cytoneme-mediated morphogen gradients by in silico modeling. *PLOS Comput. Biol.*, 17:1–30, 2021. doi: 10.1371/journal.pcbi.1009245.

[11] S. Fancher and A. Mugler. Diffusion vs. direct transport in the precision of morphogen readout. *eLife*, 9:e58981, 2020. doi: 10.7554/eLife.58981.

[12] A. Eldar, D. Rosin, B.-Z. Shilo, and N. Barkai. Self-Enhanced Ligand Degradation Underlies Robustness of Morphogen Gradients. *Dev. Cell*, 5:635–646, 2003. doi: 10.1016/S1534-5807(03)00292-2.

[13] A. D. Lander, W.-C. Lo, Q. Nie, and F. Y. M. Wan. The Measure of Success: Constraints, Objectives, and Tradeoffs in Morphogen-mediated Patterning. *CSH Perspect. Biol.*, 1:a002022, 2009. doi: 10.1101/cshperspect.a002022.

[14] Y. Song and C. Hyeon. Cost-precision trade-off relation determines the optimal morphogen gradient for accurate biological pattern formation. *eLife*, 10:e70034, 2021. doi: 10.7554/eLife.70034.

[15] T. Oosterveen, S. Kurdija, M. Enstero, C. W. Uhde, M. Bergsland, M. Sandberg, R. Sandberg, J. Muhr, and J. Ericson. SoxB1-driven transcriptional network underlies neural-specific interpretation of morphogen signals. *Proc. Natl. Acad. Sci. U.S.A.*, 110:7330–7335, 2013. doi: 10.1073/pnas.1220010110.

[16] L. Wolpert. Positional information and the spatial pattern of cellular differentiation. *J. Theor. Biol.*, 25:1–47, 1969. doi: 10.1016/S0022-5193(69)80016-0.

[17] H. Greenfeld, J. Lin, and M. C. Mullins. The BMP signaling gradient is interpreted through concentration thresholds in dorsal-ventral axial patterning. *PLoS Biol.*, 19:e3001059, 2021. doi: 10.1371/journal.pbio.3001059.

[18] K. W. Rogers, M. ElGamacy, B. M. Jordan, and P. Muller. Optogenetic investigation of BMP target gene expression diversity. *eLife*, 9:e58641, 2020. doi: 10.7554/eLife.58641.

[19] J. Jaeger and B. Verd. Dynamic positional information: Patterning mechanism versus precision in gradient-driven systems. *Curr. Top. Dev. Biol.*, 137:219–246, 2020. doi: 10.1016/bs.ctdb.2019.11.017.

[20] R. Bakker, M. Mani, and R. W. Carthew. The Wg and Dpp morphogens regulate gene expression by modulating the frequency of transcriptional bursts. *eLife*, 9:e56076, 2020. doi: 10.7554/eLife.56076.

[21] G. Williaume, S. de Buyl, C. Sirour, N. Haupaix, R. Bettoni, K. S. Imai, Y. Satou, G. Dupont, C. Hudson, and H. Yasuo. Cell geometry, signal dampening, and a bimodal transcriptional response underlie the spatial precision of an erk-mediated embryonic induction. *Dev. Cell*, 56:2966–2979 e10, 2021. doi: 10.1016/j.devcel.2021.09.025.

[22] N. Balaskas, A. Ribeiro, J. Panovska, E. Dessaud, N. Sasai, K. M. Page, J. Briscoe, and V. Ribes. Gene Regulatory Logic for Reading the Sonic Hedgehog Signaling Gradient in the Vertebrate Neural Tube. *Cell*, 148:273–284, 2012. doi: 10.1016/j.cell.2011.10.047.

[23] P. K. Grant, G. Szep, O. Patange, J. Halatek, V. Coppard, A. Csikasz-Nagy, J. Haseloff, J. C. W. Locke, N. Dalchau, and A. Phillips. Interpretation of morphogen gradients by a synthetic bistable circuit. *Nat. Commun.*, 11:5545, 2020. doi: 10.1038/s41467-020-19098-w.

[24] I. Barbier, R. Perez-Carrasco, and Y. Schaerli. Controlling spatiotemporal pattern formation in a concentration gradient with a synthetic toggle switch. *Mol. Syst. Biol.*, 16:e9361, 2020. doi: 10.15252/msb.20199361.

[25] K. Exelby, E. Herrera-Delgado, L. Garcia Perez, R. Perez-Carrasco, A. Sagner, V. Metzis, P. Sollich, and J. Briscoe. Precision of Tissue Patterning is Controlled by Dynamical Properties of Gene Regulatory Networks. *Development*, 148:dev197566, 2021. doi: 10.1242/dev.197566.

[26] M. L. Perkins. Implications of diffusion and time-varying morphogen gradients for the dynamic positioning and precision of bistable gene expression boundaries. *PLOS Comput. Biol.*, 17:1–25, 2021. doi: 10.1371/journal.pcbi.1008589.

[27] F. Xiong, A. R. Tentner, P. Huang, A. Gelas, K. R. Mosaliganti, L. Souhait, N. Rannou, I. A. Swinburne, N. D. Obholzer, P. D. Cowgill, A. F. Schier, and S. G. Megason. Specified Neural Progenitors Sort to form Sharp Domains after Noisy Shh Signaling. *Cell*, 153:550–561, 2013. doi: 10.1016/j.cell.2013.03.023.

[28] Y. Akieda, S. Ogamino, H. Furuie, S. Ishitani, R. Akiyoshi, J. Nogami, T. Masuda, N. Shimizu, Y. Ohkawa, and T. Ishitani. Cell competition corrects noisy Wnt morphogen gradients to achieve robust patterning in the zebrafish embryo. *Nat. Commun.*, page 4710, 2019. doi: 10.1038/s41467-019-12609-4.

[29] T. Y.-C. Tsai, M. Sikora, P. Xia, T. Colak-Champollion, H. Knaut, Heisenberg, C.-P., and S. G. Megason. An adhesion code ensures robust pattern formation during tissue morphogenesis. *Science*, 370:113–116, 2020. doi: 10.1126/science.aba6637.

[30] A. S. Eritano, C. L. Bromley, A. Bolea Albero, L. Schutz, F. L. Wen, M. Takeda, T. Fukaya, M. M. Sami, T. Shibata, S. Lemke, and Y. C. Wang. Tissue-Scale Mechanical Coupling Reduces Morphogenetic Noise to Ensure Precision during Epithelial Folding. *Dev. Cell*, 53:212–228 e12, 2020. doi: 10.1016/j.devcel.2020.02.012.

[31] E. Martin, S. Theis, G. Gay, B. Monier, C. Rouvière, and M. Suzanne. Mechanical control of morphogenetic robustness in an inherently challenging environment. *BioRxiv*, 2021. doi: 10.1101/2020.01.06.896266.

[32] L. Bocanegra-Moreno, A. Singh, E. Hannezo, M. Zagorski, and A. Kicheva. Cell cycle dynamics controls fluidity of the developing mouse neuroepithelium. *BioRxiv*, 2022. doi: 10.1101/2022.01.20.477048.

[33] F. He, Y. Wen, J. Deng, X. Lin, L. J. Lu, R. Jiao, and J. Ma. Probing Intrinsic Properties of a Robust Morphogen Gradient in *Drosophila*. *Dev. Cell*, 15:558–567, 2008. doi: 10.1016/j.devcel.2008.09.004.

[34] T. Bollenbach, P. Pantazis, A. Kicheva, C. Bökel, M. González-Gaitán, and F. Jülicher. Precision of the Dpp gradient. *Development*, 135:1137–1146, 2008. doi: 10.1242/dev.012062.

[35] M. D. Petkova, G. Tkačik, W. Bialek, E. F. Wieschaus, and T. Gregor. Optimal Decoding of Cellular Identities in a Genetic Network. *Cell*, 176:844–855.e15, 2019. doi: 10.1016/j.cell.2019.01.007.

[36] G. Tkačik and T. Gregor. The many bits of positional information. *Development*, 148:dev176065, 2021. doi: 10.1242/dev.176065.

[37] R. Vetter and D. Iber. Precision of morphogen gradients in neural tube development. *Nat. Commun.*, 13:1145, 2022. doi: 10.1038/s41467-022-28834-3.

[38] J. Desponds, M. Vergassola, and A. M. Walczak. A mechanism for *hunchback* promoters to readout morphogenetic positional information in less than a minute. *eLife*, 9: e49758, 2020. doi: 10.7554/eLife.49758.

[39] J. A. Adelmann, R. Vetter, and D. Iber. Impact of cell size on morphogen gradient precision. *BioRxiv*, 2022. doi: 10.1101/2022.02.02.478800.

[40] H. F. Gómez, M. S. Dumond, L. Hodel, R. Vetter, and D. Iber. 3D cell neighbour dynamics in growing pseudostratified epithelia. *eLife*, 10:e68135, 2021. doi: 10.7554/eLife.68135.

[41] Z. Zhang, S. Zwick, E. Loew, J. S. Grimley, and S. Ramanathan. Mouse embryo geometry drives formation of robust signaling gradients through receptor localization. *Nat. Commun.*, 10:4516, 2019. doi: 10.1038/s41467-019-12533-7.

[42] T. Gore, Ta. Matusek, G. D'Angelo, C. Giordano, T. Tognacci, L. Lavenant-Staccini, C. Rabouille, and P. P. Thérond. The GTPase Rab8 differentially controls the long- and short-range activity of the Hedgehog morphogen gradient by regulating Hedgehog apico-basal distribution. *Development*, 148:dev191791, 2021. doi: 10.1242/dev.191791.

[43] P. Muller, K. W. Rogers, S. R. Yu, M. Brand, and A. F. Schier. Morphogen transport. *Development*, 140:1621–1638, 2013. doi: 10.1242/dev.083519.

[44] M. Saade, I. Gutierrez-Vallejo, G. Le Dreau, M. A. Rabadan, D. G. Miguez, J. Buceta, and E. Marti. Sonic Hedgehog Signaling Switches the Mode of Division in the Developing Nervous System. *Cell Rep.*, 4:492–503, 2013. doi: 10.1016/j.celrep.2013.06.038.

[45] A. Gritli-Linde, M. Bei, R. Maas, X. M. Zhang, A. Linde, and A. P. McMahon. Shh signaling within the dental epithelium is necessary for cell proliferation, growth and polarization. *Development*, 129:5323–5337, 2002. doi: 10.1242/dev.00100.

[46] L. Legoff, H. Rouault, and T. Lecuit. A global pattern of mechanical stress polarizes cell divisions and cell shape in the growing *Drosophila* wing disc. *Development*, 140: 4051–4059, 2013. doi: 10.1242/dev.090878.

[47] R. S. Kadzik, E. D. Cohen, M. P. Morley, K. M. Stewart, M. M. Lu, and E. E. Morrisey. Wnt ligand/Frizzled 2 receptor signaling regulates tube shape and branch-point formation in the lung through control of epithelial cell shape. *Proc. Natl. Acad. Sci. U.S.A.*, 111:12444–12449, 2014. doi: 10.1073/pnas.1406639111.

[48] C. Norden. Pseudostratified epithelia - cell biology, diversity and roles in organ formation at a glance. *J. Cell Sci.*, 130:1859–1863, 2017. doi: 10.1242/jcs.192997.

[49] H. Nunley, X. Xue, J. Fu, and D. K. Lubensky. Generation of fate patterns via intercellular forces. *BioRxiv*, 2021. doi: 10.1101/2021.04.30.442205.

[50] K. S. Stapornwongkul, M. de Gennes, L. Cocconi, G. Salbreux, and J.-P. Vincent. Patterning and growth control in vivo by an engineered GFP gradient. *Science*, 370:321–327, 2020. doi: 10.1126/science.abb8205.

[51] J. Shen, F. Liu, and C. Tang. Scaling dictates the decoder structure. *BioRxiv*, 2021. doi: 10.1101/2021.03.04.433820.

[52] M. Zecca and G. Struhl. A unified mechanism for the control of Drosophila wing growth by the morphogens Decapentaplegic and Wingless. *PLOS Biol.*, 19:e3001111, 2021. doi: 10.1371/journal.pbio.3001111.

[53] S. Matsuda, J. V. Schaefer, Y. Mii, Y. Hori, D. Bieli, M. Taira, A. Plückthun, and M. Affolter. Asymmetric requirement of Dpp/BMP morphogen dispersal in the Drosophila wing disc. *Nat. Commun.*, 12:6435, 2021. doi: 10.1038/s41467-021-26726-6.

[54] M. Romanova-Michaelides, Z. Hadjivasiliou, D. Aguilar-Hidalgo, D. Basagiannis, C. Seum, M. Dubois, F. Jülicher, and M. González-Gaitán. Morphogen gradient scaling by recycling of intracellular Dpp. *Nature*, 602:287–293, 2022. doi: 10.1038/s41586-021-04346-w.

[55] S. Toda, W. L. McKeithan, T. J. Hakkinen, P. Lopez, O. D. Klein, and W. A. Lim. Engineering synthetic morphogen systems that can program multicellular patterning. *Science*, 370:327–331, 2020. doi: 10.1126/science.abc0033.

[56] A. Dupin, L. Aufinger, I. Styazhkin, F. Rothfischer, B. Kaufmann, S. Schwarz, N. Galensowske, H. Clausen-Schaumann, and F. C. Simmel. Synthetic cell-based materials extract positional information from morphogen gradients. *Sci. Adv.*, 8:eabl9228, 2022. doi: 10.1126/sciadv.abl9228.

[57] P. Van Liedekerke, J. Neitsch, T. Johann, E. Warmt, I. Gonzalez-Valverde, S. Hoehme, S. Grosser, J. Kaes, and D. Drasdo. A quantitative high-resolution computational mechanics cell model for growing and regenerating tissues. *Biomech. Model. Mechanobiol.*, 19:189–220, 2020. doi: 10.1007/s10237-019-01204-7.